Available online at http://scik.org

Commun. Math. Biol. Neurosci. 2025, 2025:128

https://doi.org/10.28919/cmbn/9550

ISSN: 2052-2541

A DYNAMICAL MODEL OF PNEUMONIA TRANSMISSION IN CHILDREN UNDER FIVE YEARS WITH NUTRITIONAL FACTORS

ARUM QURROTULAINI PRADJNA PARAMITA[1,*], RATNA HERDIANA[2,*], SUSILO HARIYANTO[2]

[1]Magister of Mathematics, Diponegoro University, Semarang, Indonesia

[2]Department of Mathematics, Diponegoro University, Semarang, Indonesia

Abstract: Pneumonia is a major cause of death among children under five in Indonesia. This study presents a mathematical model to describe the transmission dynamics of pneumonia in this age group, incorporating the effects of nutritional status. A compartmental SVITR model (Susceptible–Vaccinated–Infected–Treated–Recovered or Immune) is formulated using a system of differential equations. Model parameters are estimated using the nonlinear least squares method and calibrated using pneumonia case data from Central Java Province, covering the period from January 2022 to December 2024. The mathematical analysis involves examining the positivity and boundedness of solutions, identifying equilibrium points, computing the basic reproduction number $\mathfrak{R}_0$, and conducting local stability analysis. To identify key factors influencing disease spread, a sensitivity analysis is performed using the normalized forward sensitivity index. Numerical simulations indicate that when $\mathfrak{R}_0 < 1$, the disease does not spread endemically and will eventually die out. Sensitivity analysis reveals that nutritional improvement has the most significant impact in reducing $\mathfrak{R}_0$, followed by vaccination and antibiotic treatment, highlighting nutrition-based intervention as a key strategy for controlling pneumonia in under-five children.

Keywords: equilibrium point; numerical simulation; sensitivity analysis; SVITR model; under-five pneumonia.

2020 AMS Subject Classification: 37N25, 37C75, 93B35.

*Corresponding authors

E-mail addresses: arum.qurrotulaini@gmail.com, ratnaherdiana@lecturer.undip.ac.id

Received August 12, 2025

1. INTRODUCTION

Pneumonia is an inflammatory condition of the lung tissue caused by bacteria, fungi, protozoa, or viruses. The most common causative agent is the bacterium *Streptococcus pneumoniae* [1]. Inflammation in the lungs due to infection leads to fluid accumulation in the alveoli, impairing respiratory function. Transmission occurs through airborne droplets released when an infected individual coughs, sneezes, or talks. Indirect transmission can also occur when contaminated droplets land on surfaces, and other individuals touch these surfaces and subsequently touch their nose or mouth. Additionally, pneumonia may be transmitted vertically from mother to child during childbirth [2].

Pneumonia is the leading infectious cause of death in children aged 0–59 months worldwide. According to the World Health Organization (WHO), approximately 14% of global deaths among children under five in 2019 were attributed to pneumonia [3]. In 2023, it remained the primary cause of under-five mortality in Indonesia, accounting for 522 deaths [4]. These figures highlight the urgent need for effective control strategies, particularly for vulnerable age groups such as young children. In Indonesia, Central Java ranked third in the highest number of under-five pneumonia cases in 2023, reporting 55.232 cases, following West Java (102.576) and East Java (75.199) [4]. The high prevalence in Central Java makes it a suitable focus for this study in understanding the dynamics of pneumonia transmission among young children.

Preventive measures against pneumonia in children include vaccination, adequate nutrition, and the adoption of healthy hygiene practices. A robust immune system enables children to resist infection, whereas malnutrition and related conditions—such as lack of exclusive breastfeeding, premature birth, incomplete immunization, and co-infections like HIV or measles—can compromise immunity and increase susceptibility [3]. Infected children are typically treated with antibiotics [4].

Mathematical modeling provides a framework for representing and analyzing real-world problems using mathematical formulations. In infectious disease dynamics, such models help understand changes over time in susceptible, infected, and recovered subpopulations through differential equations. The classical SIR (Susceptible–Infected–Recovered) model introduced by Kermack and McKendrick [5] laid the foundation for disease transmission modeling. Bahaye et al. [6] extended this model to study pneumonia transmission by dividing the population into children and adults while incorporating nutritional status. Their findings, supported by Ndendya et al. [7], emphasize the heightened vulnerability of malnourished children to pneumonia. A study

conducted at the Christian University of Indonesia Hospital also found a correlation between nutritional status and pneumonia severity: 51% of 82 under-five pneumonia patients were classified as severely malnourished based on WHO growth charts [8]. These results underscore the importance of nutrition in determining both susceptibility and disease severity.

Other studies have expanded the SIR model by incorporating antibiotic treatment compartments [9][10], while vaccination has also proven effective in reducing pneumonia incidence. Several researchers have developed SVIR models to analyze the effect of vaccination strategies on disease transmission dynamics. Liu et al. [11] proposed two SVIR models to evaluate continuous and pulse vaccination strategies and demonstrated threshold dynamics based on the basic reproduction number. Zhu et al. [12] studied the global stability and optimal vaccination control in an SVIR framework, emphasizing the importance of vaccine effectiveness and immune waning. Widyaningsih et al. [13] applied an SVIR model to simulate pneumonia transmission and assess the effectiveness of vaccination in Indonesia. Optimal control approaches have also been explored within the SVIR framework in several studies [14][15], focusing on strategies to minimize infection levels and intervention costs through vaccination and social measures. These studies confirm that vaccination significantly influences transmission patterns and when effectively implemented, can lead to disease eradication. Building upon the framework by Bahaye et al. [6], this study proposes an extended SVITR (Susceptible–Vaccinated–Infected–Treated–Recovered) model by adding vaccination (V) and treatment (T) compartments while incorporating nutritional factors. The model is analyzed by determining equilibrium points and conducting numerical simulations. Furthermore, to the best of the authors' knowledge, limited studies have focused on modeling the dynamics of pneumonia among under-five children in Central Java while accounting for nutritional factors. This research seeks to provide new insights into the role of nutrition in pneumonia transmission and support the development of effective nutrition-based intervention strategies for disease control.

2. SVITR MODEL

The mathematical model analyzed in this study consists of five compartments, representing under-five children who are susceptible (S), vaccinated with PCV (V), infected with pneumonia (I), receiving antibiotic treatment (T), and recovered/immune (R). The under-five population is assumed to be closed. The structure of the model is illustrated in Figure 1.

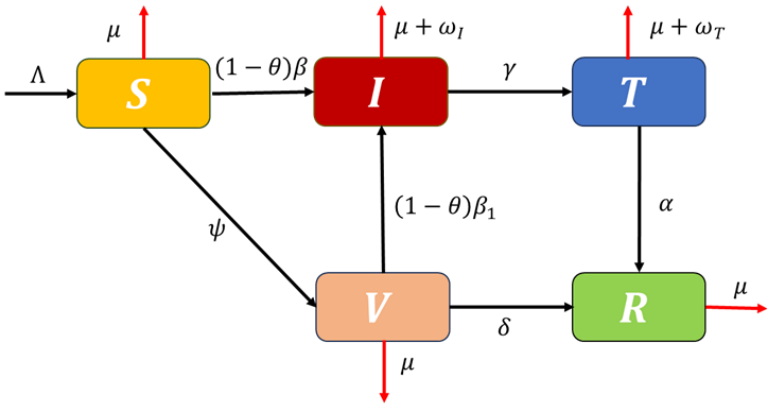

FIGURE 1. Flow Diagram of the SVITR Model for Pneumonia Dynamics

It is assumed that the total under-five subpopulation is denoted by $N(t)$, where $N(t) = S(t) + V(t) + I(t) + T(t) + R(t)$. The system of differential equations presented in Equation (1) is derived from the flow diagram shown in Figure 1.

$$
\begin{aligned}
\frac{dS}{dt} &= \Lambda - ((1-\theta)\beta I + \psi + \mu)S \\
\frac{dV}{dt} &= \psi S - (\mu + \delta)V - (1-\theta)\beta_1 VI \\
\frac{dI}{dt} &= (1-\theta)\beta SI + (1-\theta)\beta_1 VI - (\mu + \omega_I + \gamma)I \\
\frac{dT}{dt} &= \gamma I - (\mu + \omega_T + \alpha)T \\
\frac{dR}{dt} &= \delta V + \alpha T - \mu R
\end{aligned} \tag{1}
$$

with initial conditions $S(0) > 0, V(0) \geq 0, I(0) \geq 0, T(0) \geq 0, R(0) \geq 0$.

Descriptions of the model parameters are provided in Table 1. According to [16], the number of children under five years old in Central Java Province in January 2022 was recorded at 2,443,282 individuals. The birth rate parameter (Λ) is assumed to represent the number of newborns entering the under-five age group each month. This value is estimated by dividing the total number of children under five by the life expectancy (assumed to be 70 years), and then multiplying the result by 12 to convert it into a monthly rate [17-19]. Meanwhile, the natural death rate (μ) is defined as the probability of natural death per individual per month. It is calculated as the reciprocal of life expectancy (in months), by dividing one by the product of 70 years and 12 months [17-19]. The remaining model parameters are estimated using reported pneumonia case data in children under five from January 2022 to December 2024 in Central Java Province. These

estimates are obtained through a calibration process using the nonlinear least squares method.

TABLE 1. Description of model parameters

Parameter	Description	Values	Units	Source
Λ	Birth rate	$\frac{2{,}443{,}282}{70 \times 12} = 2{,}908.669$	individuals/month	Derived
β	Transmission rate from susceptible to infected	0.00001	month^{-1}	Estimated
β_1	Transmission rate from vaccinated to infected	0.000005	month^{-1}	Estimated
θ	Nutrition intervention rate	0.7	unitless	[6]
ψ	Vaccination rate	0.1351	month^{-1}	Estimated
δ	Rate of acquiring immunity after vaccination	0.6537	month^{-1}	Estimated
μ	Natural death rate	$\frac{1}{70 \times 12} = 0.0011904$	month^{-1}	Derived
ω_I	Disease-induced death rate before treatment	0.001667	month^{-1}	[19]
ω_T	Disease-induced death rate after treatment	0.0011907	month^{-1}	[9]
γ	Antibiotic treatment rate	0.9439	month^{-1}	Estimated
α	Recovery rate after receiving antibiotics	0.0011907	month^{-1}	Estimated

3. POSITIVITY AND BOUNDEDNESS ANALYSIS OF THE SOLUTIONS

To ensure that the system of ordinary differential equations is mathematically and biologically well-defined, it is necessary to prove that the solutions of System (1) remain positive and bounded [20], as stated in Theorem 1 and Theorem 2.

Theorem 1. $S(0) > 0, V(0) \geq 0, I(0) \geq 0, T(0) \geq 0, R(0) \geq 0$. *Then the solutions* $(t), V(t)$, $I(t), T(t)$, *and* $R(t)$ *of System (1) remain non-negative for all* $t \geq 0$.

Proof. Consider the first equation of System (1), given by:

$$\frac{dS}{dt} = \Lambda - ((1-\theta)\beta I + \psi + \mu)S$$

$$\frac{dS}{dt} + ((1-\theta)\beta I + \psi + \mu)S = \Lambda.$$

Let $k = (1-\theta)\beta I + \psi + \mu > 0$, then we obtain:

$$\frac{dS}{dt} + kS = \Lambda$$

This linear differential equation can be solved using the integrating factor method. Multiplying both sides by the integrating factor $e^{\int k(t)dt}$, we have:

$$\frac{dS}{dt}e^{\int k(t)dt} + kSe^{\int k(t)dt} = \Lambda\, e^{\int k(t)dt}$$
$$\frac{d}{dt}\left[S \cdot e^{\int k(t)dt}\right] = \Lambda\, e^{\int k(t)dt}$$

Integrating both sides gives:

$$S(t) \cdot e^{\int k(t)dt} = \int \Lambda\, e^{\int k(t)dt}\, dt + C$$
$$S(t) = e^{-\int k(t)dt}\left(\int \Lambda\, e^{\int k(t)dt}\, dt + C\right)$$
$$S(t) = Ce^{-\int k(t)dt} + e^{-\int k(t)dt}\int \Lambda\, e^{\int k(t)dt}\, dt$$

Or equivalently:

$$S(t) = S(0)e^{-\int_0^t k(t)\,dt} + e^{-\int_0^t k(t)\,dt}\int_0^t \Lambda\, e^{\int_0^t k(t)\,dt}\, dt \geq 0, \forall t \geq 0.$$

Therefore, $S(t)$ remains non-negative for all $t \geq 0$.

Using a similar approach, it can be shown that the functions $V(t)$, $I(t), T(t)$ and $R(t)$ are also non-negative for all $t \geq 0$. Hence, the solutions $S(t), V(t)$, $I(t), T(t)$and $R(t)$ of System (1) are non-negative for all $t \geq 0$. ■

Theorem 2. *The feasible region* Ω *defined by*

$$\Omega = \left\{(S(t), V(t), I(t), T(t), R(t)) \in \mathbb{R}_+^5 | 0 \leq S(t) + V(t) + I(t) + T(t) + R(t) \leq \frac{\Lambda}{\mu}\right\}$$

is positively invariant for the system of equations (1) with initial conditions in $\mathbb{R}_+^5$.

Proof. For each subpopulation $S(t), V(t), I(t), T(t), R(t)$ and for $t > 0$, define the total population as $N(t) = S(t) + V(t) + I(t) + T(t) + R(t)$ so that the derivative becomes:

$$\begin{aligned}
\frac{dN}{dt} &= \frac{dS}{dt} + \frac{dV}{dt} + \frac{dI}{dt} + \frac{dT}{dt} + \frac{dR}{dt} \\
&= \Lambda - \big((1-\theta)\beta I + \psi + \mu\big)S + \psi S - (\mu + \delta)V - (1-\theta)\beta_1 VI + (1-\theta)\beta S \\
&+ (1-\theta)\beta_1 VI - (\mu + \omega_I + \gamma)I + \gamma I - (\mu + \omega_T + \alpha)T + \delta V + \alpha T - \mu R \\
&= \Lambda - (1-\theta)\beta SI - \psi S - \mu S + \psi S - \mu V - \delta V - (1-\theta)\beta_1 VI + (1-\theta)\beta S \\
&+ (1-\theta)\beta_1 VI - \mu I - \omega_I I - \gamma I + \gamma I - \mu T - \omega_T T - \alpha T + \delta V + \alpha T - \mu R \\
&= \Lambda - \mu S - \mu V - \mu I - \omega_I I - \mu T - \omega_T T - \mu R \\
&= \Lambda - \mu(S + V + I + T + R) - \omega_I I - \omega_T T \\
&= \Lambda - \mu N - \omega_I I - \omega_T T \\
&\leq \Lambda - \mu N
\end{aligned}$$

From the inequality above, we obtain the differential inequality:

$$\frac{dN(t)}{dt} + \mu N(t) \leq \Lambda$$

Multiplying both sides by the integrating factor $e^{\int_0^t \mu(t)dt}$, we get:

$$\frac{dN(t)}{dt} \cdot e^{\int_0^t \mu(t)dt} + \mu N(t) \cdot e^{\int_0^t \mu(t)dt} \leq \Lambda \cdot e^{\int_0^t \mu(t)dt}$$

$$\frac{d}{dt}[N \cdot e^{\mu t}] \leq \Lambda \cdot e^{\mu t}$$

$$N(t) \cdot e^{\mu t} \leq \int_0^t \Lambda \cdot e^{\mu t}\, dt + N(0)$$

$$N(t) \cdot e^{\mu t} - N(0) \leq \left[\frac{\Lambda}{\mu} \cdot e^{\mu t}\right]_0^t$$

$$N(t) \cdot e^{\mu t} \leq \frac{\Lambda}{\mu} e^{\mu t} - \frac{\Lambda}{\mu} + N(0)$$

$$N(t) \leq \frac{\Lambda}{\mu} + \left(N(0) - \frac{\Lambda}{\mu}\right) e^{-\mu t}$$

As $t \to \infty$, it follows that $N(t) \leq \frac{\Lambda}{\mu}$. Therefore, each subpopulation remains bounded above, and the feasible region Ω is positively invariant. ■

4. EQUILIBRIUM POINTS AND BASIC REPRODUCTION NUMBER

Based on the model described in System of Equations (1), the equilibrium points can be obtained by setting the system's derivatives to zero, i.e. cara $\frac{dS}{dt} = 0, \frac{dV}{dt} = 0, \frac{dI}{dt} = 0, \frac{dT}{dt} = 0$ and $\frac{dR}{dt} = 0$ which yields the following system:

$$\begin{aligned} 0 &= \Lambda - ((1-\theta)\beta I + \psi + \mu)S \\ 0 &= \psi S - (\mu + \delta)V - (1-\theta)\beta_1 VI \\ 0 &= (1-\theta)\beta SI + (1-\theta)\beta_1 VI - (\mu + \omega_I + \gamma)I \\ 0 &= \gamma I - (\mu + \omega_T + \alpha)T \\ 0 &= \delta V + \alpha T - \mu R. \end{aligned} \tag{2}$$

In the study of disease dynamics, two types of equilibrium points are commonly identified: the disease-free equilibrium and the endemic equilibrium.

4.1. Disease-Free Equilibrium (DFE)

DFE occurs when there is no disease transmission in the population. By setting $I = 0$ and $T = 0$ in the System (2), we obtain the DFE as follows:

$$E^0 = (S^0, V^0, I^0 T^0, R^0) = \left(\frac{\Lambda}{\psi + \mu}, \frac{\Lambda\psi}{(\mu + \delta)(\psi + \mu)}, 0, 0, \frac{\Lambda\psi\delta}{\mu(\mu + \delta)(\psi + \mu)}\right).$$

This equilibrium is particularly useful for computing the basic reproduction number ($\Re_0$), which quantifies the average number of secondary infections generated by a single infected individual in a completely susceptible population. The value of $\Re_0$ is determined using the Next Generation Matrix (NGM) approach, by computing the spectral radius of the matrix product $F \cdot V^{-1}$, where F represents the rate of appearance of new infections and V the rate of transitions among infected compartments [21].

Let $= [I, T]^t$, then the system can be rewritten as $\dot{x} = \mathcal{F} + \mathcal{V}$, with:

$$\dot{x} = \begin{bmatrix} (1-\theta)\beta IS + (1-\theta)\beta_1 VI - (\mu + \omega_I + \gamma)I \\ \gamma I - (\mu + \omega_T + \alpha)T \end{bmatrix}$$

$$\mathcal{F} = \begin{bmatrix} \mathcal{F}_1 \\ \mathcal{F}_2 \end{bmatrix} = \begin{bmatrix} (1-\theta)\beta IS + (1-\theta)\beta_1 VI \\ 0 \end{bmatrix}$$

Since there are no new infections directly caused by the variable T, it follows that $\mathcal{F}_2 = 0$.

$$\mathcal{V} = \begin{bmatrix} \mathcal{V}_1 \\ \mathcal{V}_2 \end{bmatrix} = \begin{bmatrix} (\mu + \omega_I + \gamma)I \\ -\gamma I + (\mu + \omega_T + \alpha)T \end{bmatrix}$$

The matrices F and V represent the Jacobian matrices of $\mathcal{F}$ and $\mathcal{V}$, respectively, evaluated at the disease-free equilibrium point.

$$F = \begin{pmatrix} \frac{(1-\theta)\Lambda\,((\mu + \delta)\beta + \beta_1\psi)}{(\mu + \delta)(\psi + \mu)} & 0 \\ 0 & 0 \end{pmatrix}$$

$$V = \begin{pmatrix} (\mu + \omega_I + \gamma) & 0 \\ -\gamma & (\mu + \omega_T + \alpha) \end{pmatrix}$$

Thus, the basic reproduction number is given by:

$$\Re_0 = \rho(F \cdot V^{-1}) = \frac{\Lambda(1-\theta)\,(\beta(\mu + \delta) + \beta_1\psi)}{(\mu + \delta)(\psi + \mu)(\mu + \omega_I + \gamma)}.$$

4.2. Endemic Equilibrium (EE)

The endemic equilibrium occurs when the disease persists in the population over time. Solving the full nonlinear system yields the endemic equilibrium $E^* = (S^*, V^*, I^*, T^*, R^*)$, where:

$$S^* = \frac{\Lambda}{(C_1 I^* + C_3)},$$

$$V^* = \frac{\psi\Lambda}{(C_1I^* + C_3)(C_4 + C_2I^*)},$$

$$I^* = \frac{-(C_1C_4C_6 + C_2C_6 - \Lambda C_1C_2) + \sqrt{(C_1C_4C_6 + C_2C_6 - \Lambda C_1C_2)^2 - 4(C_1C_2C_6)(C_3C_4C_6 + \Lambda C_1C_4)}}{2[C_1C_2C_6]},$$

$$T^* = \frac{\gamma I^*}{C_5},$$

$$R^* = \frac{\delta\psi\Lambda}{\mu(C_1I^* + C_3)(C_4 + C_2I^*)} + \frac{\alpha\gamma I^*}{\mu C_5}.$$

The reproduction number can also be expressed in terms of the constants C_i as

$$\Re_0 = \frac{\Lambda(C_1C_4 + C_2\psi)}{C_3C_4C_6}$$

where

$$C_1 = (1-\theta)\beta > 0,$$
$$C_2 = (1-\theta)\beta_1 > 0,$$
$$C_3 = (\psi + \mu) > 0,$$
$$C_4 = (\mu + \delta) > 0,$$
$$C_5 = (\mu + \omega_T + \alpha) > 0,$$
$$C_6 = (\mu + \omega_I + \gamma) > 0.$$

5. LOCAL STABILITY ANALYSIS

To analyze the local stability of the DFE, the Jacobian matrix of the system will be evaluated at that point. The local stability criterion is determined by the sign of the eigenvalues of the Jacobian matrix. If all eigenvalues have negative real parts, then the disease-free equilibrium is locally asymptotically stable.

Theorem 3. *Let* $\Re_0 = \frac{\Lambda(C_1C_4+C_2\psi)}{C_3C_4C_6}$. *The DFE* $E^0 = \left(\frac{\Lambda}{C_3}, \frac{\Lambda\psi}{C_3C_4}, 0, 0, \frac{\Lambda\psi\delta}{\mu C_3C_4}\right)$ *is locally asymptotically stable if* $\Re_0 < 1$.

Proof. Linearization of System (1) is performed using the first-order Taylor series expansion, resulting in the Jacobian matrix of the system:

$$J = \begin{bmatrix} -C_1I - C_3 & 0 & -C_1S & 0 & 0 \\ \psi & -C_4 - C_2I & -C_2V & 0 & 0 \\ C_1I & C_2I & C_2V - C_6 & 0 & 0 \\ 0 & 0 & \gamma & -C_5 & 0 \\ 0 & \delta & 0 & \alpha & -\mu \end{bmatrix}$$

Next, the DFE is substituted into the Jacobian matrix

$$J(E^0) = \begin{bmatrix} -C_3 & 0 & -\frac{\Lambda C_1}{C_3} & 0 & 0 \\ \psi & -C_4 & -\frac{\Lambda\psi C_2}{C_3 C_4} & 0 & 0 \\ 0 & 0 & \frac{\Lambda\psi C_2}{C_3 C_4} - C_6 & 0 & 0 \\ 0 & 0 & \gamma & -C_5 & 0 \\ 0 & \delta & 0 & \alpha & -\mu \end{bmatrix}$$

The eigenvalues of the Jacobian matrix are obtained by solving the characteristic equation $\det(\lambda I - J(E^0)) = 0$. This gives:

$$\left| \begin{bmatrix} \lambda & 0 & 0 & 0 & 0 \\ 0 & \lambda & 0 & 0 & 0 \\ 0 & 0 & \lambda & 0 & 0 \\ 0 & 0 & 0 & \lambda & 0 \\ 0 & 0 & 0 & 0 & \lambda \end{bmatrix} - \begin{bmatrix} -C_3 & 0 & -\frac{\Lambda C_1}{C_3} & 0 & 0 \\ \psi & -C_4 & -\frac{\Lambda\psi C_2}{C_3 C_4} & 0 & 0 \\ 0 & 0 & \frac{\Lambda\psi C_2}{C_3 C_4} - C_6 & 0 & 0 \\ 0 & 0 & \gamma & -C_5 & 0 \\ 0 & \delta & 0 & \alpha & -\mu \end{bmatrix} \right| = 0$$

$$\Leftrightarrow \left| \begin{bmatrix} \lambda + C_3 & 0 & \frac{\Lambda C_1}{C_3} & 0 & 0 \\ -\psi & \lambda + C_4 & \frac{\Lambda\psi C_2}{C_3 C_4} & 0 & 0 \\ 0 & 0 & \lambda + C_6 - \frac{\Lambda\psi C_2}{C_3 C_4} & 0 & 0 \\ 0 & 0 & -\gamma & \lambda + C_5 & 0 \\ 0 & -\delta & 0 & -\alpha & \lambda + \mu \end{bmatrix} \right| = 0$$

The characteristic equation is obtained as:

$$(3) \qquad \left((\lambda + C_3)(\lambda + C_4)(\lambda + C_5)(\lambda + \mu)\left(\lambda + C_6 - \frac{\Lambda\psi C_2}{C_3 C_4}\right)\right) = 0$$

The roots of Equation (3) are:

$$\lambda_1 = -C_3,$$
$$\lambda_2 = -C_4,$$
$$\lambda_3 = -C_5$$
$$\lambda_4 = -\mu,$$
$$\lambda_5 = -C_6 + \frac{\Lambda\psi C_2}{C_3 C_4} \Leftrightarrow \lambda_5 = -C_6 + \frac{\Re_0 C_3 C_4 C_6 - \Lambda C_1 C_4}{C_3 C_4} \Leftrightarrow \lambda_5 = -C_6 + \Re_0 C_6 - \frac{\Lambda C_1}{C_3}$$
$$\Leftrightarrow \lambda_5 = (\Re_0 - 1)C_6 - \frac{\Lambda C_1}{C_3}$$

Since C_1, C_3, C_4, C_5, C_6 and μ are all positive constants, it follows that $\lambda_1, \lambda_2, \lambda_3, \lambda_4$ are negative. For $\Re_0 < 1$, the fifth eigenvalue λ_5 is also negative. Hence, all eigenvalues have negative real parts, which implies that the disease-free equilibrium point is locally asymptotically stable when $\Re_0 < 1$. ■

6. SENSITIVITY ANALYSIS OF PARAMETERS

The purpose of parameter sensitivity analysis is to determine how much the parameters of $\Re_0$ influence the value of $\Re_0$. The magnitude of this influence can be identified through the parameter sensitivity index. The normalized forward sensitivity index is a sensitivity analysis method used to understand how much a change in a parameter affects a particular variable [22]. The normalized forward sensitivity index for a variable $u = \Re_0$, which depends differentially on parameter p, is defined as:

$$S_p^u = \frac{\partial u}{\partial p} \cdot \frac{p}{u} \tag{4}$$

where

S_p^u : ensitivity index of variable u with respect to parameter p

$\frac{\partial u}{\partial p}$: Change in u due to a small change in parameter p

$\frac{p}{u}$: Normalization factor to ensure that sensitivity results are on the same scale, making it easier to compare across parameters.

The results of the sensitivity index calculations for the parameters of $\Re_0$ using Equation (4) are shown in Table 2 and Figure 2 below.

TABLE 2. Sensitivity index of parameters for $u = \Re_0$

Parameter (p)	**Sensitivity values** (S_p^u)
Λ	$+1$
θ	-2.3333
β	$+0.9064$
β_1	$+0.0935$
μ	-0.0101
δ	-0.0933
γ	-0.9969
ω_I	-0.0017
ψ	-0.8977

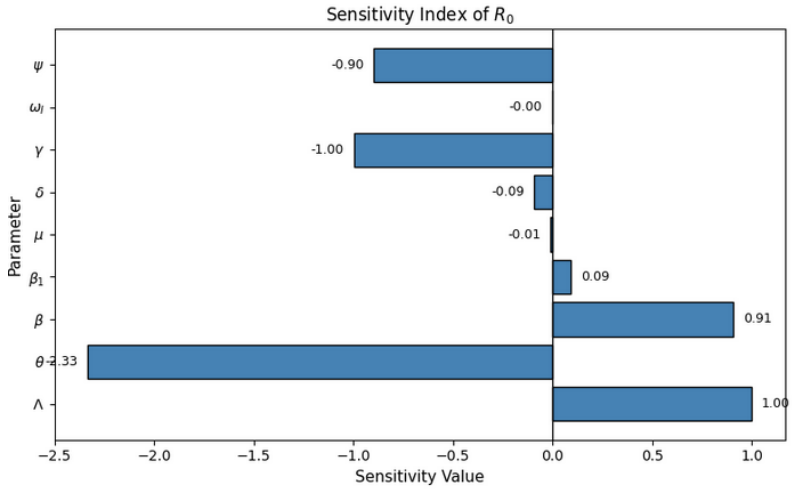

FIGURE 2. Diagram of the Normalized Forward Sensitivity Index for the SVITR Model of Pneumonia

Based on the sensitivity indices, it is found that the parameter with the most significant negative impact on $\mathfrak{R}_0$ is θ, with a value of -2.3333. This means that a 1% increase in the nutrition intervention rate will reduce $\mathfrak{R}_0$ by 2.3333%. In other words, improving nutritional support can reduce the potential transmission of pneumonia among children under five. In addition to θ, other parameters that negatively influence $\mathfrak{R}_0$ are ψ, ω_I, γ, δ and μ, with respective sensitivity indices of -0.8977, -0.0017, -0.9969, -0.0933 and -0.0101. This indicates that increasing the vaccination rate, disease-induced death rate before treatment, antibiotic treatment rate, rate of acquiring immunity after vaccination and natural death rate can reduce the potential for disease spread. On the other hand, parameters that positively affect $\mathfrak{R}_0$ are Λ, β and β_1 with a sensitivity index of +1, +0.9064, and +0.0935. Sensitivity index of +1 shows that a 1% increase in the birth rate will contribute to a 1% increase in the potential spread of pneumonia among children under five.

Contour plots and surface plots are presented to illustrate the relationship between two key parameters and changes in the basic reproduction number $\mathfrak{R}_0$. These visualizations help identify parameter combinations that most significantly influence the dynamics of pneumonia transmission among children under five. The contour plot displays contour lines representing constant values of $\mathfrak{R}_0$. The color intensity and density of the lines reflect the level of sensitivity—tighter contour lines indicate that small changes in the parameters lead to substantial changes in $\mathfrak{R}_0$. This plot helps distinguish between safe zones (where $\mathfrak{R}_0 < 1$) and high-risk zones (where $\mathfrak{R}_0 > 1$) based on variations in parameter values. Meanwhile, the surface plot provides a three-dimensional perspective, showing how $\mathfrak{R}_0$ responds to simultaneous changes in two parameters. Steep

surfaces indicate high sensitivity, meaning that even slight changes in the parameters can result in significant shifts in $\mathfrak{R}_0$. This visualization is useful for evaluating intervention strategies, such as increasing vaccination rates or improving nutritional support, and their potential impact on reducing disease spread.

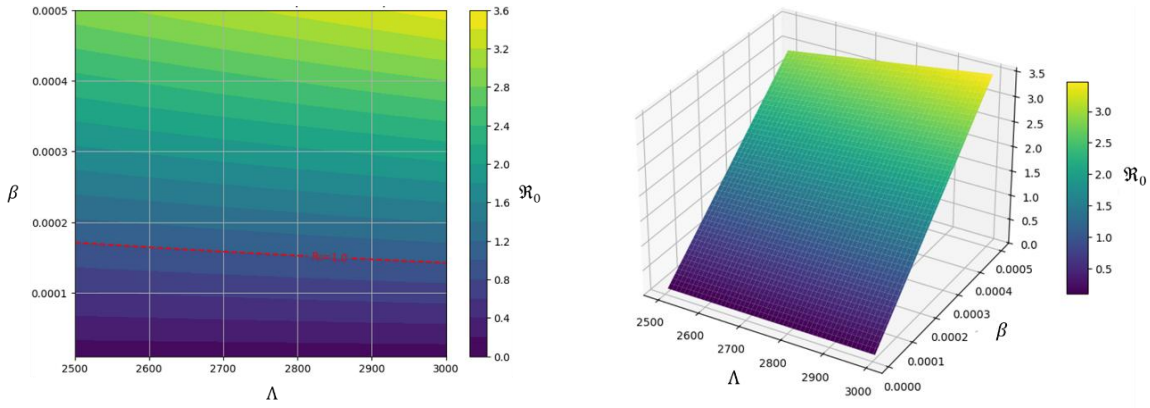

(a) (b)

FIGURE 3. Contour Plot and Surface Plot of $\mathfrak{R}_0$ with Respect to Λ and β

In Figure 3(a), the contour plot shows that the basic reproduction number $\mathfrak{R}_0$ increases significantly with higher values of β, whereas variations in Λ only result in minor changes in $\mathfrak{R}_0$. The dense contour lines along the β -axis indicate high sensitivity to this parameter. Meanwhile, the surface plot in Figure 3(b) reinforces this observation by showing a steep gradient in the β direction, creating a sharp surface, while the Λ axis remains relatively flat. This suggests that disease transmission is more strongly influenced by the transmission rate (β) than by the recruitment rate of susceptible individuals (Λ).

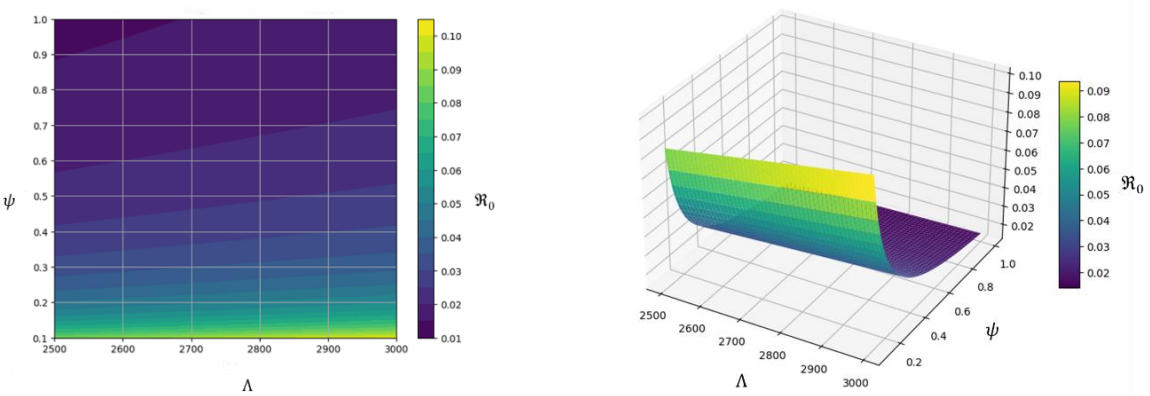

(a) (b)

FIGURE 4. Contour Plot and Surface Plot of $\mathfrak{R}_0$ with Respect to Λ and ψ

The contour plot in Figure 4(a) shows that an increase in ψ (the vaccination rate) drastically reduces $\mathfrak{R}_0$, as indicated by the dense and sharply downward-curving contour lines. In contrast,

an increase in Λ has only a minor impact. The surface plot in Figure 4(b) depicts a steep decline of the surface in the direction of ψ, illustrating the effectiveness of vaccination in controlling disease transmission, even as the number of susceptible individuals increases. Vaccination intervention is shown to be highly significant in reducing the basic reproduction number.

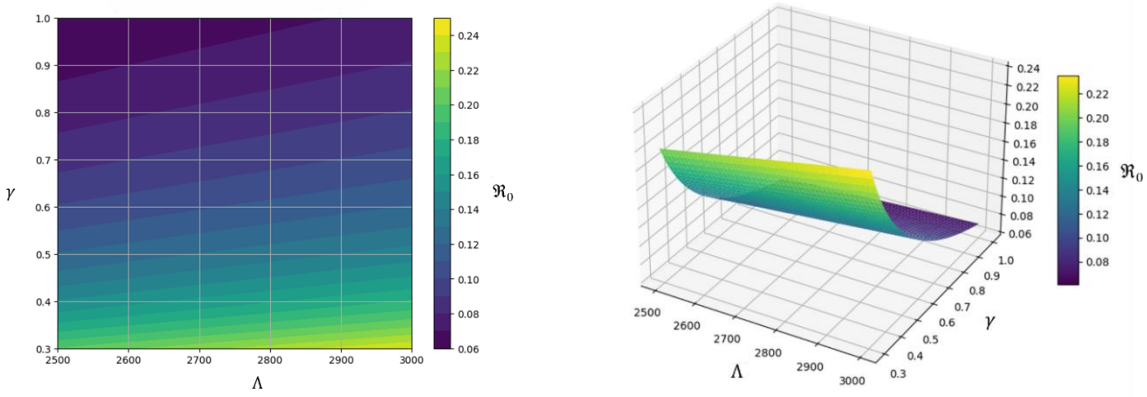

(a) (b)

FIGURE 5. Contour Plot and Surface Plot of $\mathfrak{R}_0$ with Respect to Λ and γ

Figure 5(a) shows that $\mathfrak{R}_0$ increases with higher recruitment of susceptible individuals (Λ), while a higher recovery rate (γ) consistently lowers $\mathfrak{R}_0$. The color gradient reveals that γ has a strong effect—boosting γ significantly reduces $\mathfrak{R}_0$, even when Λ is high. This trend is confirmed in the surface plot of Figure 5(b), where $\mathfrak{R}_0$ sharply declines as γ increases. In contrast, the influence of Λ is more gradual and less impactful. These results highlight that improving recovery through treatment is a key strategy to reduce disease spread, even when the number of susceptible individuals grows.

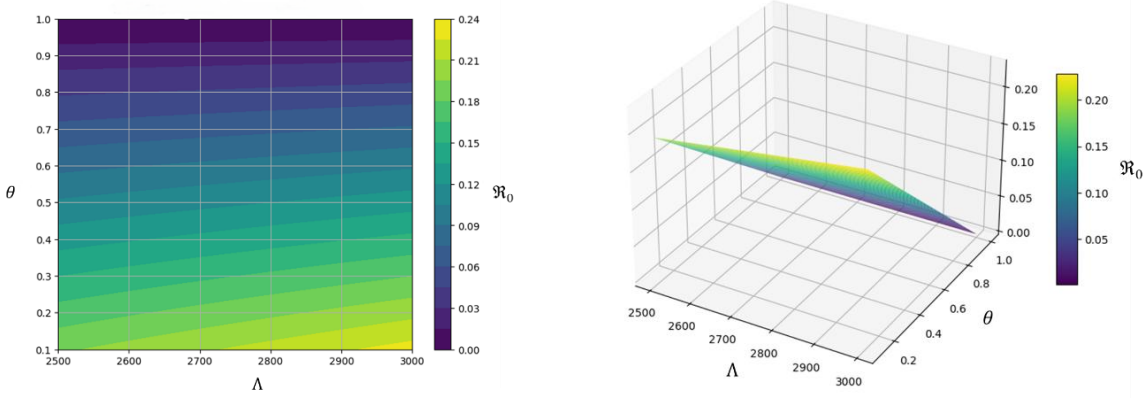

(a) (b)

FIGURE 6. Contour Plot and Surface Plot of $\mathfrak{R}_0$ with Respect to Λ and θ

Figure 6(a) shows that $\mathfrak{R}_0$ tends to increase with a higher recruitment rate of susceptible individuals (Λ), while a higher nutrition intervention rate (θ) consistently reduces $\mathfrak{R}_0$. The color

gradient on the contour plot indicates that θ has a strong effect, especially at low to moderate levels. Even when Λ is high, increasing θ still leads to a gradual decline in $\mathfrak{R}_0$. This suggests that improved nutrition can effectively curb disease transmission, even as Λ grows. The surface plot in Figure 6(b) confirms this trend, showing a sharp drop in $\mathfrak{R}_0$ as θ increases. In contrast, Λ shows a more linear and less steep effect. Enhancing nutritional support appears to be an effective strategy to reduce transmission, even under conditions of high population recruitment.

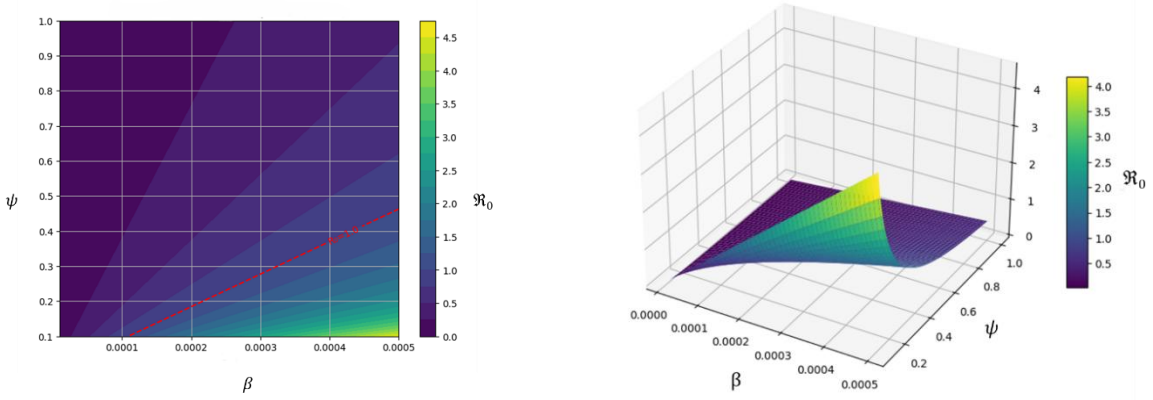

(a) (b)

FIGURE 7. Contour Plot and Surface Plot of $\mathfrak{R}_0$ with Respect to β and ψ

Figure 7(a) shows that $\mathfrak{R}_0$ increases sharply with higher transmission rates (β), while higher vaccination rates (ψ) consistently lower $\mathfrak{R}_0$. The contour plot highlights β as a dominant factor, especially when ψ is low. However, even at high β, increasing ψ significantly reduces $\mathfrak{R}_0$, keeping it within a safer range. The red dashed line in the plot marks a threshold for policy decisions. Figure 7(b) reinforces this pattern with a steep rise in the $\mathfrak{R}_0$ surface as β increases, particularly when ψ is low. As ψ rises, the surface flattens, showing that vaccination effectively dampens disease spread. Reducing transmission and increasing vaccination are both crucial and complementary strategies for lowering $\mathfrak{R}_0$ and controlling the outbreak.

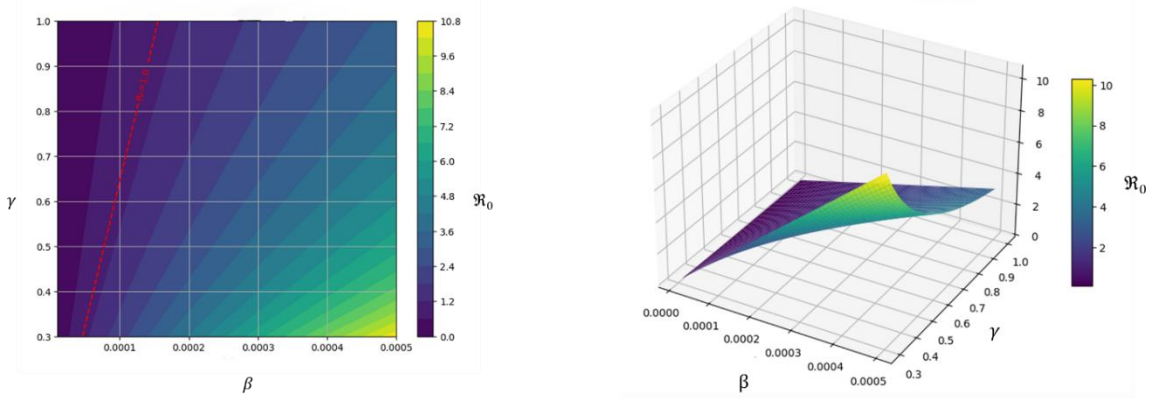

(a) (b)

FIGURE 8. Contour Plot and Surface Plot of $\mathfrak{R}_0$ with Respect to β and γ

Figure 8(a) shows that $\mathfrak{R}_0$ increases with a higher transmission rate (β), while a higher antibiotic treatment rate (γ) consistently lowers it. The contour plot indicates that increasing γ has a strong suppressing effect on $\mathfrak{R}_0$, especially when moving from low to moderate values. In contrast, increasing β causes a steep rise in $\mathfrak{R}_0$, particularly when γ is low. The red dashed line at $\mathfrak{R}_0 = 1$ marks the epidemic threshold—values below it suggest controlled transmission, while values above signal a potential outbreak. Figure 8(b) confirms this pattern: the $\mathfrak{R}_0$ surface rises sharply with β, especially at low γ, but flattens as γ increases. This shows that while both parameters significantly affect $\mathfrak{R}_0$, they do so differently— β drives it up exponentially, while γ reduces it gradually but effectively. Reducing transmission and increasing antibiotic treatment are complementary strategies to keep $\mathfrak{R}_0$ below the epidemic threshold.

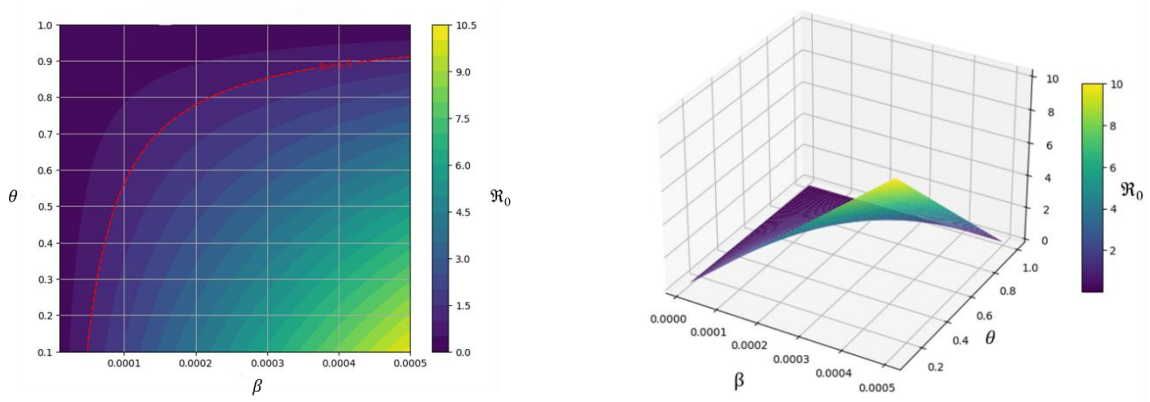

(a) (b)

FIGURE 9. Contour Plot and Surface Plot of $\mathfrak{R}_0$ with Respect to β and θ

Figure 9(a) shows that the $\mathfrak{R}_0$ rises sharply with an increase in the transmission rate (β), while a higher nutrition intervention rate (θ) consistently reduces $\mathfrak{R}_0$. The contour plot illustrates that $\mathfrak{R}_0$ is highly sensitive to changes in β, especially when θ is low. However, increasing θ gradually lowers $\mathfrak{R}_0$, even when β remains high. Figure 9(b) confirms this trend: the $\mathfrak{R}_0$ surface rises steeply with higher β, especially at low θ, but flattens as θ increases. This suggests that improved nutrition can effectively suppress disease spread. In summary, reducing β and enhancing nutrition (θ) work together to keep $\mathfrak{R}_0$ under control. Nutritional interventions act as a protective factor, helping to slow or even prevent transmission, especially in high-risk scenarios.

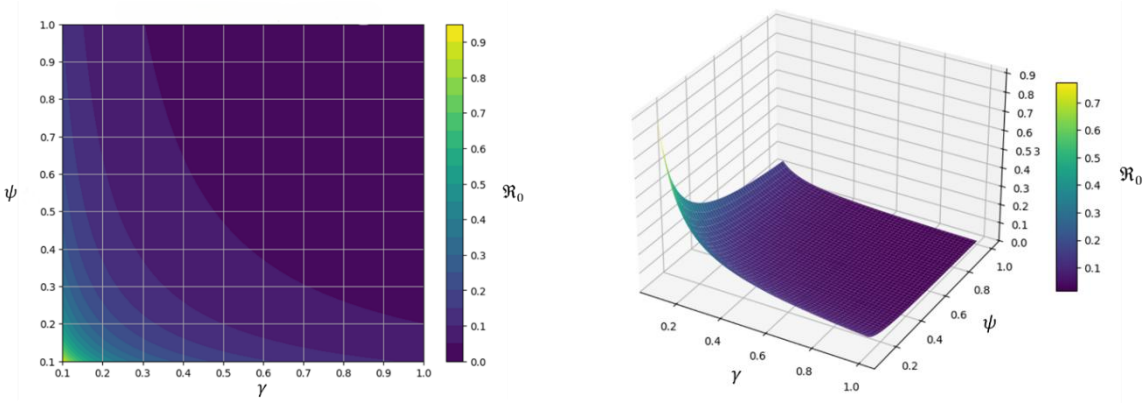

(a) (b)

FIGURE 10. Contour Plot and Surface Plot of $\mathfrak{R}_0$ with Respect to γ and ψ

Figure 10(a) shows that the $\mathfrak{R}_0$ significantly decreases as both the antibiotic treatment rate (γ) and vaccination rate (ψ) increase. The contour plot reveals that the most substantial drop in $\mathfrak{R}_0$ occurs when both γ and ψ increase from low to moderate levels. As these values continue to rise, $\mathfrak{R}_0$ approaches zero, suggesting that disease transmission can be effectively suppressed through this combined intervention. In Figure 10(b), surface plot of $\mathfrak{R}_0$ drops steeply in the lower corner (low γ and ψ) and flattens as both parameters increase, indicating that even modest improvements in treatment and vaccination can drastically reduce disease spread. Increasing antibiotic treatment and vaccination rates is a highly effective strategy to reduce $\mathfrak{R}_0$ to safe levels and potentially stop disease transmission altogether.

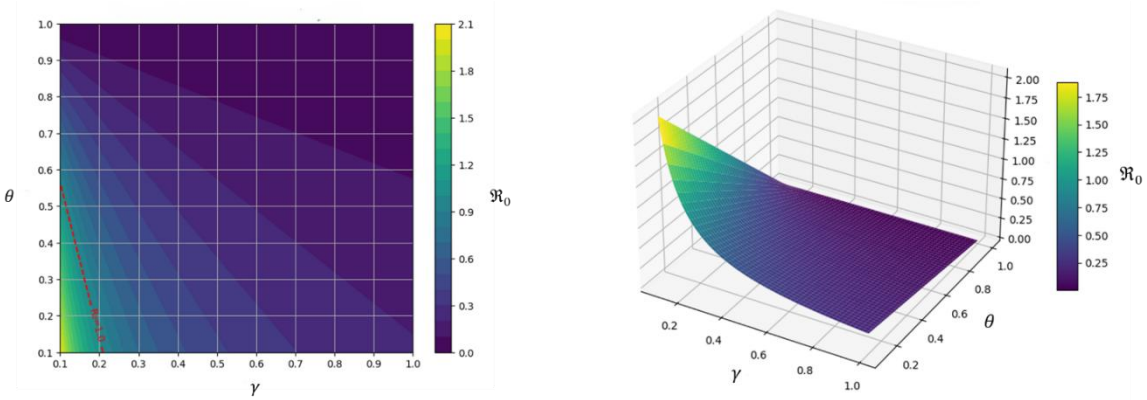

(a) (b)

FIGURE 11. Contour Plot and Surface Plot of $\mathfrak{R}_0$ with Respect to γ and θ

Figure 11(a) shows that the $\mathfrak{R}_0$ decreases significantly as both the antibiotic treatment rate (γ) and the nutrition intervention rate (θ) increase. The contour plot indicates that $\mathfrak{R}_0$ is high when both parameters are low but drops sharply when either or both increase. The dashed red line at

$\mathfrak{R}_0 = 1$ marks a critical threshold between uncontrolled and controllable disease spread. Figure 11(b) reinforces this finding. The surface plot of $\mathfrak{R}_0$ is steep at low γ and θ values but becomes flatter as both parameters increase, highlighting their combined effect in reducing transmission. Overall, the results suggest that improving access to antibiotics and nutritional support can work together to reduce $\mathfrak{R}_0$ to safe levels, making this combination an effective strategy to control and prevent outbreaks—especially in vulnerable populations.

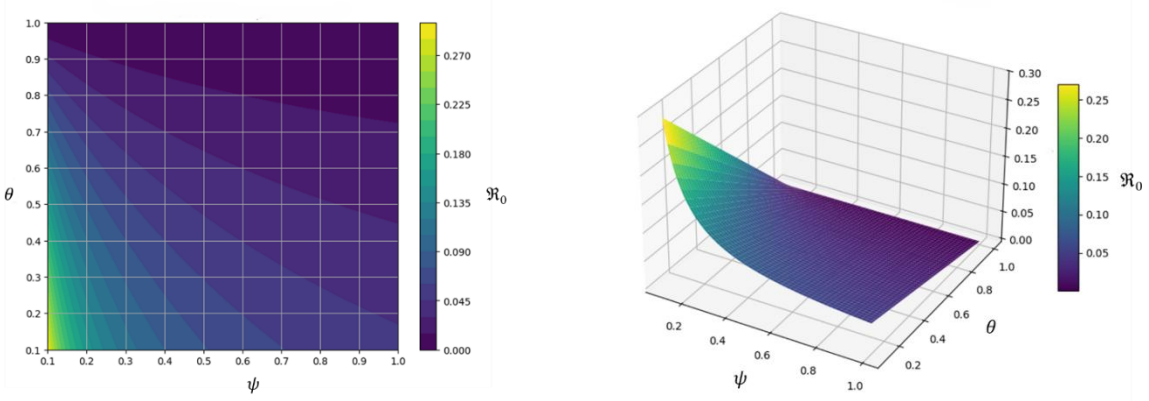

(a) (b)

FIGURE 12. Contour Plot and Surface Plot of $\mathfrak{R}_0$ with Respect to ψ and θ

Figure 12(a) shows that the $\mathfrak{R}_0$ gradually decreases as both the vaccination rate (ψ) and the nutrition intervention rate (θ) increase. The contour plot reveals that $\mathfrak{R}_0$ is highest when both ψ and θ are low but steadily declines as either parameter rises. Figure 12(b) confirms this trend through a surface plot, where $\mathfrak{R}_0$ drops sharply at low values of ψ and θ, then flattens out as both parameters increase. This suggests a synergistic effect: combining vaccination with improved nutrition can significantly reduce $\mathfrak{R}_0$, even when the initial transmission risk is moderate. Strengthening immunization programs and improving nutrition are effective combined strategies for preventing disease spread in the population.

7. NUMERICAL SIMULATION

In the numerical simulation, pneumonia case data among children under five from the Central Java Provincial Health Office [19] were applied to the system of equations (1). The initial values for each compartment variable in January 2022 are $S(0) = 2{,}242{,}049, V(0) = 191{,}112, I(0) = 3{,}816, T(0) = 3{,}434$ and $R(0) = 2{,}871$. Based on the estimated parameter values presented in Table 1 and the initial conditions of the under-five subpopulation in Central Java Province, a numerical simulation was carried out using the fourth-order Runge-Kutta method to examine the transmission dynamics of pneumonia. The results of the simulation are illustrated in Figure 3.

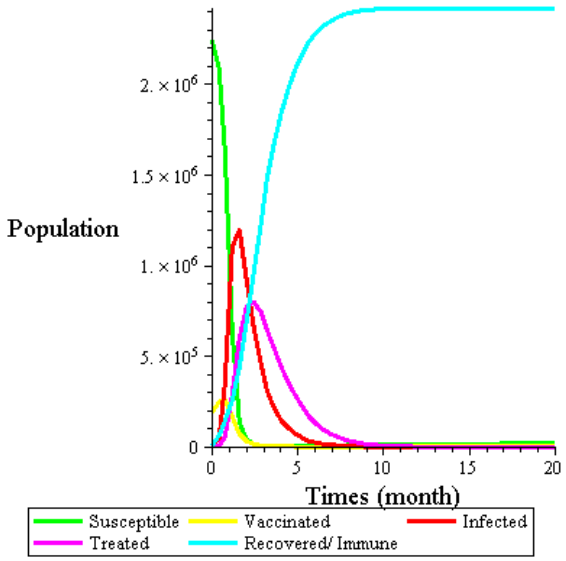

FIGURE 13. Numerical Simulation of the DFE with $\Re_0 = 0.0746 < 1$

As shown in Figure 13, the basic reproduction number $\Re_0 = 0.0746 < 1$ indicates that pneumonia does not spread endemically within the under-five subpopulation. This is evidenced by the curve representing infected individuals, which exhibits a brief spike at approximately $t = 1.5$ months, reaching a peak of 1,248,390 infected individuals. After this point, the number of infections decreases rapidly, approaching zero without oscillation, which implies that the infection is not sustained in the long term.

The simulation results support this theoretical prediction. The system reaches a steady state at approximately $t = 14.6$ months, characterized by all compartment values approaching constants. The values at this equilibrium point from the simulation are

$S = 16,593,\ V = 3,171,\ I = 11,\ T = 203$ and $R = 2,415,458.$

These values are compared with the theoretical DFE, derived analytically as

$S^0 = 21,345,\ V^0 = 4{,}404,\ I^0 = 0,\ T^0 = 0$ and $R^0 = 2,418,791.$

At $t = 14.6$ month, the differences between the numerical approximation and the theoretical results are within an acceptable ranges. The total population at equilibrium in the simulation is $2{,}436{,}436$, while theoretically it is $2{,}444{,}540$ yielding a difference of only 0.33%. The numerical simulation confirm that the system tends asymptotically toward the DFE as $t \to \infty$ and support the theoretical conclusion that, under the condition $\Re_0 < 1$, the DFE is locally asymptotically stable. The stability implies that pneumonia will eventually be eliminated from the under-five population in Central Java, provided that current health interventions, such as vaccination, antibiotic treatment, and nutritional programs, are maintained or improved.

8. CONCLUSION

The SVITR model represents the dynamics of pneumonia transmission among children under five, consists of five compartments: susceptible, vaccinated, infected, treated, and recovered/immune subpopulations. In this study, the effect of nutritional intervention for children is taken into account and represented by the parameter θ. Based on analytical calculations, it is shown that the disease-free equilibrium point is locally asymptotically stable when $\Re_0 < 1$. This is supported by numerical simulations using monthly pneumonia case data among children under five in Central Java Province from January 2022 to December 2024. The numerical simulations confirm the theoretical analysis, indicating that when $\Re_0 < 1$, the disease does not spread widely and tends to die out in the long term. The sensitivity analysis results show that nutritional intervention can reduce the potential for disease transmission.

CONFLICT OF INTERESTS

The authors declare that there is no conflict of interests.

REFERENCES

[1] A. Morimura, S. Hamaguchi, Y. Akeda, K. Tomono, Mechanisms Underlying Pneumococcal Transmission and Factors Influencing Host-Pneumococcus Interaction: A Review, Front. Cell. Infect. Microbiol. 11 (2021), 639450. https://doi.org/10.3389/fcimb.2021.639450.

[2] B.M. Huber, P.M. Meyer Sauteur, W.W. Unger, P. Hasters, M.R. Eugster, et al., Vertical Transmission of Mycoplasma Pneumoniae Infection, Neonatology 114 (2018), 332-336. https://doi.org/10.1159/000490610.

[3] WHO, Pneumonia in Children, World Health Organization, (2025). https://www.who.int/news-room/fact-sheets/detail/pneumonia.

[4] Ministry of Health Republic of Indonesia, Indonesia Health Profile 2023, 2024. https://kemkes.go.id/eng/indonesia-health-profile-2023.

[5] W.O. Kermack, A.G. McKendrick, A Contribution to the Mathematical Theory of Epidemics, Proc. R. Soc. Lond. Ser. A 115 (1927), 700-721. https://doi.org/10.1098/rspa.1927.0118..

[6] D.W. Bahaye, T. Marijani, G. Mlay, An Age-Structured Differential Equations Model for Transmission Dynamics of Pneumonia with Treatment and Nutrition Intervention, Healthc. Anal. 4 (2023), 100279. https://doi.org/10.1016/j.health.2023.100279.

[7] J.Z. Ndendya, Y.A. Liana, Mathematical Model and Analysis of Pneumonia on Children Under Five Years with Malnutrition, SSRN (2024). https://doi.org/10.2139/ssrn.4692559.

[8] A. Adriani, V.P. Simarmata, The Relationship Between Nutritional Status and Degree of Pneumonia in Toddlers at Universitas Kristen Indonesia General Hospital, J. Drug Deliv. Ther. 12 (2022), 129-133. https://doi.org/10.22270/jddt.v12i3-s.5391.

[9] C. Chukwu, S. Tchoumi, M. Diagne, A Simulation Study to Assess the Epidemiological Impact of Pneumonia Transmission Dynamics in High-Risk Populations, Decis. Anal. J. 10 (2024), 100423. https://doi.org/10.1016/j.dajour.2024.100423.

[10] B.S. kotola, T.T. Mekonnen, Mathematical Model Analysis and Numerical Simulation for Codynamics of Meningitis and Pneumonia Infection with Intervention, Sci. Rep. 12 (2022), 2639. https://doi.org/10.1038/s41598-022-06253-0.

[11] X. Liu, Y. Takeuchi, S. Iwami, Svir Epidemic Models with Vaccination Strategies, J. Theor. Biol. 253 (2008), 1-11. https://doi.org/10.1016/j.jtbi.2007.10.014.

[12] X. Zhu, H. Liu, X. Lin, Q. Zhang, Y. Wei, Global Stability and Optimal Vaccination Control of Svir Models, AIMS Math. 9 (2024), 3453-3482. https://doi.org/10.3934/math.2024170.

[13] P. Widyaningsih, G. Musta'in, D.R.S. Saputro, Susceptible Vaccinated Infected Recovered Model with the Exclusive Breastfeeding and Its Application to Pneumonia Data in Indonesia, BAREKENG 19 (2025), 999-1008. https://doi.org/10.30598/barekengvol19iss2pp999-1008.

[14] A. Ramponi, M.E. Tessitore, Optimal Social and Vaccination Control in the Svir Epidemic Model, Mathematics 12 (2024), 933. https://doi.org/10.3390/math12070933.

[15] H. Ismail, A. Debbouche, S. Hariharan, L. Shangerganesh, S.V. Kashtanova, Stability and Optimality Criteria for an Svir Epidemic Model with Numerical Simulation, Mathematics 12 (2024), 3231. https://doi.org/10.3390/math12203231.

[16] Central Java Province Health Office, Monthly Report on the Control of Acute Respiratory Infections in Central Java Province, Central Java Province Health Office, Semarang.

[17] R.R. Musafir, A. Suryanto, I. Darti, Dynamics of Covid-19 Epidemic Model with Asymptomatic Infection, Quarantine, Protection and Vaccination, Commun. Biomath. Sci. 4 (2021), 106-124. https://doi.org/10.5614/cbms.2021.4.2.3.

[18] R.C.A. Ariyani, Widowati, Kartono, R. Heru Tjahjana, R.H.S. Utomo, Analysis of Local Stability of the Model on Covid-19 Spread in Dki Jakarta Province, E3S Web Conf. 448 (2023), 05006. https://doi.org/10.1051/e3sconf/202344805006.

[19] D. Aldila, N. Awdinda, Fatmawati, F.F. Herdicho, M.Z. Ndii, et al., Optimal Control of Pneumonia Transmission Model with Seasonal Factor: Learning from Jakarta Incidence Data, Heliyon 9 (2023), e18096. https://doi.org/10.1016/j.heliyon.2023.e18096.

[20] R. Herdiana, H. Tjahjana, A. Henindya, N.S.A. Latif, Optimal Control of Smoking Cessation Programs for Two Subclasses of Smoker, J. Math. Comput. Sci. 31 (2023), 41-55. https://doi.org/10.22436/jmcs.031.01.04.

[21] O. Diekmann, J.A.P. Heesterbeek, M.G. Roberts, The Construction of Next-Generation Matrices for Compartmental Epidemic Models, J. R. Soc. Interface 7 (2009), 873-885. https://doi.org/10.1098/rsif.2009.0386.

[22] M. Zamir, G. Zaman, A.S. Alshomrani, Sensitivity Analysis and Optimal Control of Anthroponotic Cutaneous Leishmania, PLOS ONE 11 (2016), e0160513. https://doi.org/10.1371/journal.pone.0160513.